

# An Ultrasensitive Bioluminescent Enzyme Immunoassay Based on Nanobody/Nanoluciferase Heptamer Fusion for the Detection of Tetrabromobisphenol A in Sediment

Zhenfeng Li,<sup>||</sup> Yi Wang,<sup>||</sup> Natalia Vasylieva, Debin Wan, Zihan Yin, Jiexian Dong, and Bruce D. Hammock\*



Cite This: *Anal. Chem.* 2020, 92, 10083–10090



Read Online

ACCESS |



Metrics & More

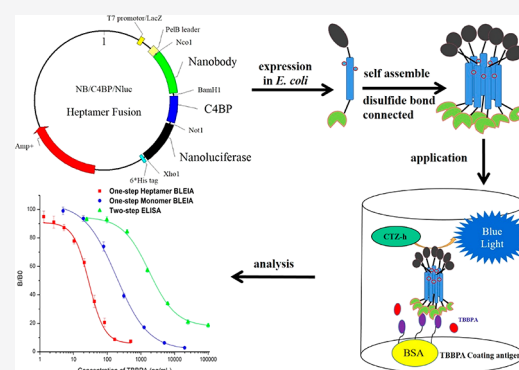


Article Recommendations



Supporting Information

**ABSTRACT:** Tetrabromobisphenol A (TBBPA) is a flame retardant and has become a widely concerning environmental pollutant. An ultrasensitive nanobody-based immunoassay was developed to monitor the exposure of TBBPA in sediment. First, the anti-TBBPA nanobody was fused with nanoluciferase, and then a one-step bioluminescent enzyme immunoassay (BLEIA) was developed with high sensitivity for TBBPA, with a maximum half inhibition concentration ( $IC_{50}$ ) at 187 pg/mL. Although approximately 10-fold higher sensitivity can be achieved by this developed BLEIA than by the classical two-step ELISA ( $IC_{50}$  at 1778 pg/mL), it is still a challenge to detect trace TBBPA in sediment samples reliably due to the relatively high matrix effect. To further improve the performance of this one-step BLEIA, a C4b-binding protein (C4BP) was inserted as a self-assembling linker between the nanobody and nanoluciferase. Therefore, a heptamer fusion containing seven binders and seven tracers was generated. This reagent improved the binding capacity and signal amplification. The one-step heptamer plus BLEIA based on this immune-reagent shows an additional 7-fold improvement of sensitivity, with the  $IC_{50}$  of 28.9 pg/mL and the limit of detection as low as 2.5 pg/mL. The proposed assay was further applied to determine the trace TBBPA in sediment, and the recovery was within 92–103%. Taking advantage of this heptamer fusion, one-step BLEIA can serve as a powerful tool for fast detection of trace TBBPA in the sediment samples.



Flame retardants were widely used as an additive in the manufacture of circuit boards, furniture textiles, and specialty papers. Tetrabromobisphenol A (TBBPA) is currently one of the world's mostly used brominated flame retardants.<sup>1</sup> Because of its wide use and environmental contamination, and potential human exposure, the toxicity of TBBPA has caused widespread concern.<sup>2–4</sup> Although it was banned in many countries, TBBPA is ubiquitous in the environment, including household dust, soil, water, sewage, sludge, and sediment.<sup>5</sup> TBBPA degrades slowly in the environment, and it can bioaccumulate in fish and aquatic invertebrates.<sup>3</sup> Thus, the pollution of TBBPA in the environment is a serious problem that needs attention. Many analytical methods used to detect TBBPA are traditional instrumental methods,<sup>6</sup> including liquid chromatography (LC) and LC–mass spectrometry (LC–MS).<sup>7</sup> Instrumental methods are highly sensitive and selective, yet require trained analysts, expensive instruments, and complicated sample pretreatments.<sup>8–10</sup> Alternatively, immunoassay based on antibodies against TBBPA is a simple and effective method for detecting TBBPA in a high-throughput manner.<sup>11</sup>

Recently, nanobodies have attracted much attention in the field of immunoassays for environmental monitoring.<sup>12</sup> It has

been reported that through strict screening procedures, from immunized alpaca, phage display, biological panning, and finally expression in *E. coli*, nanobodies against TBBPA have been successfully isolated.<sup>13</sup> As compared to the classical polyclonal antibody-based immunoassay, immunoassay based on nanobodies shows excellent, sensitive detection of TBBPA. Besides, nanobodies, as good bioengineering materials, can be fused with many reporter proteins.<sup>14</sup> For example, the anti-TBBPA nanobody has been successfully fused with an alkaline phosphatase fusion protein. One-step immunoassay based on this fusion protein has been developed to detect TBBPA in the urines<sup>15</sup> and surface soil sample.<sup>16</sup> Nanobody and nanobody fusions are resistant to many organic solvents,<sup>17</sup> so it is feasible to extract the TBBPA in different matrixes with organic solvents and directly subject the extract to a nanobody-based

Received: May 4, 2020

Accepted: June 19, 2020

Published: June 19, 2020



immunoassay. However, for an environmental sample, like sewage, sludge, and sediment samples, those samples have a stronger matrix effect in immunoassays because many components may be coextracted during sample preparation.<sup>18</sup> The extraction from these samples was usually treated with an extra cleanup procedure with a solid-phase extraction (SPE) cartridge to eliminate the matrix effect prior to immunoassay analysis.<sup>19</sup> In our previous study, the extract of TBBPA in sediment after cleanup still needed an extra 50-fold dilution prior to ELISA runs.<sup>11</sup> Indeed, the reduction of matrix interference is a challenge in an immunoassay for the detection of TBBPA in environmental samples.

Because cleanup with SPE is costly, time-consuming, and also not suitable for high-throughput, dilution with assay buffer directly was considered as a simple approach to reduce the matrix effect.<sup>20</sup> However, the limit of detection (LOD) in immunoassay is sacrificed in dilution, especially for complicated environmental samples for which 100-fold dilution may be needed.<sup>21</sup> Luckily, the loss of sensitivity during sample dilution can be compensated by changing the detection mode in the immunoassay. For example, changing from colorimetric to fluorescent detection could bring about a 10-fold sensitivity improvement.<sup>22</sup> However, the fluorescent detection mode can raise the signal-to-noise problems due to autofluorescence and self-quenching. Recently, our group published a bioluminescent immunoassay based on a nanobody/nanoluciferase fusion, which was established to detect Aflatoxin B1 with a 20-fold improvement of sensitivity when compared to classical ELISA.<sup>23</sup> Another strategy to improve sensitivity in an immunoassay is the application of multivalent antibodies with improved affinity.<sup>24</sup> A variety of multivalent antibody engineering techniques have been developed, including chemical ligation,<sup>25</sup> fusion with self-polypeptide, and heterodimer modules.<sup>26</sup> Nanobody, as a recombinant binder, is an excellent material for multivalent engineering techniques. It was reported that a nanobody linked to the B subunit of verotoxin could self-assemble to form pentamer<sup>27</sup> and decamer molecules.<sup>28</sup> The coiled-coil peptide of human cartilage oligomeric matrix protein and ferritin was also applied to make a nanobody multimer, respectively, termed as combody<sup>29</sup> and fenobody<sup>30</sup> with dramatically increased affinity. C4-binding protein (C4BP) is a spider-like structure composed of seven  $\alpha$ -chains; the amphipathic helices and two cysteine residues in the C-terminus of the C4BP have been extensively studied for their roles in polymerization.<sup>31</sup> C4BP has been reported to be suitable for the polymerization of the molecule when fused to various proteins.<sup>32,33</sup> Here, a novel platform to fuse nanobody at the N-terminal of C4BP and the nanoluciferase at the C-terminal of C4BP was proposed to create a biofunctional immune-reagent both as a high-affinity binder and as a sensitive tracer.

In the present study, our goal was to develop a multivalent nanobody-based immunoassay, which is ultrasensitive to allow at least 100-fold dilution in preparing complicated environmental samples, which highly reduces the matrix effect. Our data show that by using monomer anti-TBBPA nanobody fused with nanoluciferase, the sensitivity of one-step BLEIA was 10-fold higher than that of the classic two-step nanobody-based ELISA. To further improve the sensitivity of the one-step BLEIA, the C4BP peptide was applied to assemble a heptamer of nanobody/C4BP/Nluc fusion. The one-step BLEIA using this novel immune-reagent greatly improved

the sensitivity and compensated for the loss of sensitivity due to the dilution treatment of sediment samples.

## MATERIALS AND METHODS

**Chemicals and Methods.** The synthesis of haptens and the preparation of coating antigen were described in previous studies.<sup>13</sup> The standard substance of TBBPA was bought from TCI Co., Ltd. (Tokyo, Japan). Most of the other chemicals such as isopropyl- $\beta$ -D-thiogalactopyranoside (IPTG), bovine serum albumin (BSA), and imidazole were obtained from Sigma-Aldrich Chemical Co. (St. Louis, MO). Coelenterazine-H (CTZ-h) was purchased from NanoLight Technology ProLume Ltd. (Pinetop, AZ). All restriction enzymes and T4 DNA ligase were purchased from New England Biolabs, Inc. (Ipswich, MA). HisPur Ni-NTA resin, B-PER, Halt protease inhibitor cocktail, and Nunc white flat-bottom 96-well plates were purchased from Thermo Fisher Scientific Inc. (Rockford, IL).

**Nanobody Fused with Nanoluciferase.** According to our previous study, the best clone of anti-TBBPA nanobody (T15) was selected along with the best coating antigen T3-BSA. Plasmid pET-22b encoding nanoluciferase gene was developed in our laboratory described in the previous studies.<sup>23</sup> The gene for the T15 nanobody carried by the pComb3X vector was amplified by PCR (primers in Table S1) and cloned into the nanoluciferase harboring pET-22b plasmid using complementary *Nco*I and *Bam*HI restriction sites (Figure S1). The sequenced T15 nanobody/nanoluciferase (NB/Nluc) plasmid was transformed to BL21 (DE3) by heat shock. After the induction of expression by 0.5 mM IPTG induction, the proteins were purified with Ni-NTA resin and eluted by 150 mM imidazole in PBS (0.01 mol/L phosphate, 0.137 M NaCl, 3 M KCl, pH 7.4). Sodium dodecyl sulfate-polyacrylamide gel electrophoresis (SDS-PAGE) was employed to determine the size and purity of T15 NB/Nluc.

**Procedure of Two-Step ELISA and One-Step Nanobody-Nluc-Based BLEIA.** In this study, two formats of immunoassay were developed in a routine procedure. As shown in Figure S2, the indirect competitive two-step nanobody-based ELISA was developed in our previous work<sup>13</sup> and carried out as follows. A microtiter plate was coated with T3-BSA coating antigen (1  $\mu$ g/mL) overnight in coating buffer (pH 9.6). 3% skim milk in PBS (pH 7.4) was used for blocking at ambient temperature for 1 h. After being washed with PBST (PBS containing 0.05% Tween-20), 50  $\mu$ L of serial dilutions of TBBPA was added to each well, followed by 50  $\mu$ L of the T15 nanobody. The concentrations of coating antigen and antibody were determined by checkerboard titration. After 1 h of incubation, the plate was washed five times with PBST, and 100  $\mu$ L of anti-HA Mab-HRP was added to the well and incubated for 1 h at ambient temperature. The plate was washed three times with PBST. The TMB substrate solution was added before the plate was incubated at 37  $^{\circ}$ C for 7 min. The reaction was terminated by the addition of 50  $\mu$ L of 3 M H<sub>2</sub>SO<sub>4</sub>. The absorbance was measured with a Tecan 1000 plate reader (Tecan Inc., Research Triangle Park, NC) at 450 nm. As shown in Figure S3, the one-step NB/Nluc-based BLEIA developed in this work was carried out as described below: the concentration of coating antigen and NB/Nluc was determined by checkerboard titration. The plate was coated with T3-BSA coating antigen (0.01  $\mu$ g/mL) overnight and blocked with 3% skim milk for 1 h. After being washed with PBST, 50  $\mu$ L of serial dilutions of TBBPA and 50  $\mu$ L of the

T15 NB/Nluc fusion protein were added to the plate per well. The plate was incubated at ambient temperature for 1 h and washed. The nanoluciferase activity was determined by addition of 100  $\mu\text{L}$  of CTZ-h substrate (5  $\mu\text{g}/\text{mL}$  in ethanol) in the luminescence assay buffer (pH 8.0, 10 mmol/L PBS containing 1% Tergitol NP-10, 0.25 mg/mL BSA, and 8.8 mmol/L EDTA- $\text{Na}_2$ ). The bioluminescent signal was read in a Tecan 1000 plate reader in luminescence mode. Origin 8.5 (OriginLab, MA) was employed to generate the standard curve for both two-step ELISA and one-step BLEIA by taking the logarithm of the TBBPA standard concentration as the abscissa and the signal response as the ordinate with the four-parameter logistic fitting formula.

**Matrix Effect and Detection of TBBPA in Sediment Sample.** The one-step immunoassay based on NB/Nluc was applied to the detection of TBBPA in sediment samples collected from the creek in the campus of University of California, Davis (38.54° N, 121.76° W). The sediment sample was collected with a 5 feet long, rigid plastic tube hollow in both ends. The tube was straightly inserted to the bottom of the creek at least 0.5 feet deep, and then the sediments were air-dried in the laboratory. The total of organic carbon (TOC) and pH of the sediment were determined as  $110.52 \pm 0.03$  (g  $\text{kg}^{-1}$ ) and  $7.11 \pm 0.01$ , respectively. Matrix effects of sediment samples were evaluated following a simple dilution protocol. Briefly, 1 g of dry sediment (TBBPA free confirmed by LC-MS/MS) was directly extracted with 5 mL of water/methanol = 1/1 extraction solution, and then the extraction was diluted with assay buffers in 5-, 10-, 20-fold, respectively. The TBBPA standards were prepared by diluting the extraction solution into serial concentrations with the assay buffer and assay buffer only. One-step BLEIA based on the NB/C4BP/Nluc heptamer using these TBBPA standards was set up, and the standard curve between them was fitted and overlapped by the Origin 8.5 program to evaluate the matrix effect.

**Construction of Nanobody-C4BP-Nanoluciferase Plasmids.** The gene encoding C4BP self-assembled peptide was synthesized according to the published protein sequence.<sup>34</sup> The C4BP peptide was designed as a bridge connecting two functional domains, nanobody and nanoluciferase. As shown in Table S2, a flexible linker "GSGGGGGSGGGGSGGGGSGGGGSG" was inserted between nanobody with C4BP peptide, while another flexible linker "NSGGGSGGGTG" was inserted between the C4BP peptide and nanoluciferase. The heptamer NB/Nluc plasmid was constructed on the basis of the plasmid frame pET-22b encoding T15 NB/Nluc gene. First, the gene encoding C4BP containing flexible linkers was amplified with PCR and flanked with *Bam*HI/*Not*I using primers listed in Table S2. The plasmid was flanked with *Bam*HI/*Not*I, and the C4BP PCR products were ligated in the flanked pET-22b vector by T4 ligase. After confirmation by sequencing, the fragment C4BP was inserted as a connector linked to two functional genes to format a new fusion gene, named NB/C4BP/Nluc. The sequenced T15 NB/C4BP/Nluc plasmid was transformed into three *E. coli* hosts purchased from Millipore Sigma (Burlington, U.S.), including Tuner (DE3), BL21 (DE3), and Rosetta2 (Gami) by heat shock. The heptamer proteins were expressed and purified using the same procedure as that of the monomer proteins (NB/Nluc). The size and purity of T15 NB/C4BP/Nluc were determined by sodium dodecyl sulfate-polyacrylamide gel electrophoresis (SDS-PAGE) both in reduced and in nonreduced conditions.

**Binding Characterization of Monomer and Heptamer Fusions.** The T3-BSA coating antigen was prepared in 5-fold serial dilution with coating buffer (starting point at 1  $\mu\text{g}/\text{mL}$ ). The plate was coated with serial dilutions of T3-BSA overnight along with blank control without coating antigen and then blocked with 3% skim milk for 1 h. To compare the binding activity of monomer and heptamer fusion, the concentrations of both fusion proteins were adjusted to 0.1 mg/mL, which was confirmed by nanodrop measurement. 100  $\mu\text{L}$  per well of the diluted fusion protein was added to the plate coated with T3-BSA and incubated for 1 h. After the addition of 100  $\mu\text{L}$  of CTZ-h substrate in the luminescence assay buffer in each well, the bioluminescence intensity was measured with Tecan 1000. The potency curve was fitted by plotting the luminescence signal response against the concentration of the T3-BSA with the Origin 8.5 program. The cutoff value was calculated as the concentration with the formula  $S/N > 3$ .

The interactions between the two nanobody/nanoluciferase fusion proteins and the coating antigen T3-BSA were measured by Bio-Layer Interferometry (BLI) with Octet Qke system (Fortebio, Fremont, U.S.). The coating antigen was biotinylated and loaded on the commercial streptavidin sensor. The two fusion proteins were diluted with binding buffer in a series of four concentrations (5, 10, 20, and 40  $\mu\text{g}/\text{mL}$ , respectively). Individual sensors recorded the kinetic signals of serial dilution samples, including assay buffer as blank control. The association and dissociation phases were recorded for 185 and 300 s, respectively. The real-time interaction data were recorded with agitation at 1000 rpm during data acquisition, and individual binding curves were fitted using Octet data analysis software v9.0.

**One-Step BLEIA Based on NB/C4BP/Nluc Heptamer.** The NB/C4BP/Nluc-based BLEIA was developed in the one-step mode: the concentration of coating antigen and NB/C4BP/Nluc was determined by checkerboard titration. The plate was coated with 100  $\mu\text{L}$  of T3-BSA coating antigen (0.002  $\mu\text{g}/\text{mL}$ ) overnight, and 3% skim milk was added for blocking for 1 h. After being washed with PBST, 50  $\mu\text{L}$  of serially diluted TBBPA and 50  $\mu\text{L}$  of T15 NB/C4BP/Nluc fusion protein per well were added to the plate. The plate was incubated at ambient temperature for 1 h and washed before 100  $\mu\text{L}$  of CTZ-h substrate (5  $\mu\text{g}/\text{mL}$ ) in the luminescence assay buffer was added. The bioluminescent signal was read in a Tecan 1000 reader in luminescent mode. The luminescence signal response was plotting against the logarithm of the standard concentration of TBBPA in logistic fitting formula with the Origin 8.5 program.

**Detection of TBBPA in Sediment Sample.** For the recovery study, a series of TBBPA (0, 500, 1000, 1500, 3000, and 4000 pg) were spiked into the TBBPA free sediment (the dry weight is 1 g). The samples were first gently shaken for 10 min in 5 mL of water/methanol = 1/1 extraction solution. After centrifugation at 10 000g for 10 min, the supernatant was diluted with assay buffer and subjected directly to the one-step BLEIA based on both NB/Nluc and NB/C4BP/Nluc. The extraction solution was also subjected to the LC-MS/MS method following the centrifugation at 3000g for 20 min. The analysis by LC-MS/MS was carried out in an Agilent HPLC and 4000 Qtrap mass spectrometer along with a C18 column (Table S3).

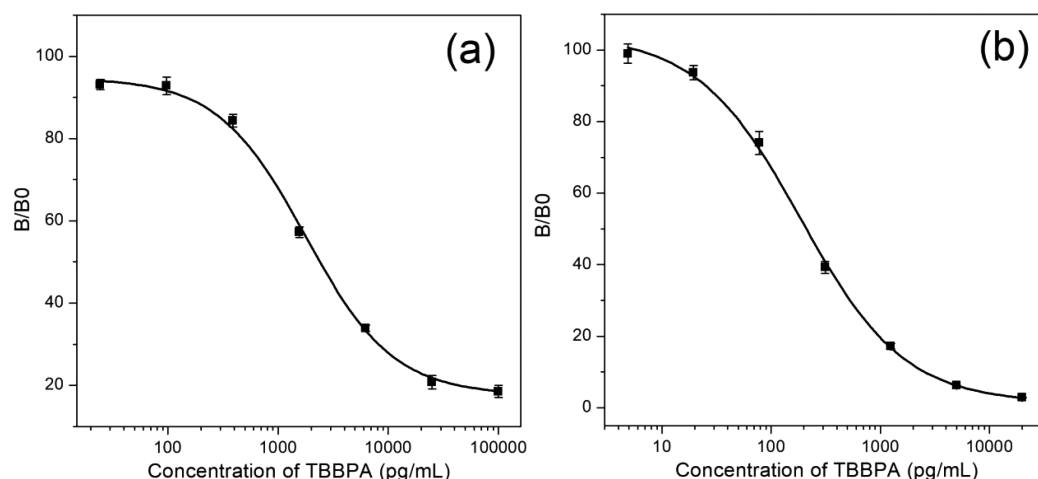


**Figure 1.** Two-step ELISA standard curve based on nanobody and anti-HA Mab-HRP tracer (a) and one-step BLEIA standard curve based on difunctional nanobody/nanoluciferase (b).

## RESULTS AND DISCUSSION

**Expression and Identification of Nanobody Nanoluciferase Fusion.** Nanobody T15 against TBBPA was obtained from an immunized alpaca derived phage display library in our previous study.<sup>13</sup> Nanoluciferase, a small reporter protein (19 kDa), is a very efficient bioluminescent enzyme used in BLEIA frequently. It has been shown that nanoluciferase is easily produced in high yield in *E. coli*, which makes it a highly attractive fusion partner. In this study, the plasmid containing nanobody/nanoluciferase fusion gene was prepared by molecular engineering. The nanobody T15 and nanoluciferase were linked with a flexible linker (GGGGS)<sup>2</sup> according to the sequencing result (Table S1). Following a standard routine, the *E. coli* harboring fusion gene was expressed and purified in a Ni-affinity column chromatography. The yield of fusion was determined as 10 mg by weight from 1 L of bacterial culture media. As shown in Figure S4, the NB/Nluc fusion protein is found as one dominant band of 40 kDa upon SDS-PAGE analysis, which indicates the expected fusion protein has been obtained successfully.

**Performance of One-Step BLEIA as Compared to Two-Step ELISA.** The NB/Nluc fusion is a bifunctional immunoreagent, which serves as a binder for recognizing the coating antigen and meanwhile a tracer to provide signal amplification in immunoassay. Thus, it is valuable for the development of one-step immunoassays. The classic two-step dc-ELISA based on nanobody T15 was also carried out to compare the sensitivity between parental nanobody and NB/Nluc fusion protein. Both the parental nanobody and the NB/Nluc fusion proteins showed excellent affinity to the coating antigens T3-BSA and inhibition by free TBBPA. Using the anti-HA-tag Mab HRP conjugated as the secondary tracer, two-step ELISA was applied for the detection of TBBPA with an IC<sub>50</sub> value of 1778 pg/mL (Figure 1a). Meanwhile, NB/Nluc, which served as binder and tracer, was applied to develop a one-step bioluminescent enzyme immunoassay (BLEIA) along with the CTZ-h substrate (Figure S2). Because of the strong signal amplification effect on nanoluciferase/CTZ-h, the concentration of T3-BSA coating antigen was drastically decreased when optimized in checkerboard titration. The developed BLEIA was almost 10 times more sensitive than the classic two-step ELISA, with an IC<sub>50</sub> value of 187 pg/mL and a limit of detection of 25.2 pg/mL (Figure 1b). Also, the

NB/Nluc fusion-based one-step immunoassay reduced the time significantly to 1 h as compared to at least 2 h for the two-step ELISA.

**Matrix Effect in the Detection of TBBPA in Sediment.** Sediment samples were collected from an organic matter-rich creek at the campus of the University of California, Davis. The sediment samples were dried and kept in a sealed container until use. The sediment samples were tested with LC-MS/MS to confirm the absence of TBBPA before the study of the matrix effect in BLEIA. Sediment (1 g) was weighed before the addition of water/methanol = 1/1 extraction solution (5 mL). The sample was then sonicated for 20 min. Finally, the supernatant was obtained by centrifuging the samples for 15 min at 3000g. One of the most common sample pretreatment methods to minimize matrix effects on immunoassay is by the dilution of sample extracts with assay buffer. In this study, the extraction solution of sediment was diluted with assay buffer 10% methanol in PBS by different factors of 5, 10, and 20. This procedure of using methanol takes advantage of the solvent resistance of the reagents to minimize the binding of the lipophilic analyte to plastic plate. As shown in Figure 2, the maximum luminescence intensity was significantly reduced among sediment samples diluted by 5- and 10-fold, which indicated the strong matrix effect in sediment. The absence of matrix effect was evidenced by the similarity between the calibration curve prepared in a diluted matrix as compared to a calibration curve generated in the assay buffer. The standard curve of 20-fold diluted extraction almost overlapped with that of the assay buffer. On the basis of the results, a 20-fold dilution was chosen as an optimal dilution for the developed assay. In our study, the sediment sample was dissolved in 5 mL of extraction solution and then diluted with assay buffer by 20-fold, which resulted in a total of 100-fold dilution before the BLEIA assay was performed. The developed BLEIA has a LOD of 25.2 pg/mL for the detection of TBBPA in assay buffer, which means a LOD of 2520 pg/g for the detection of TBBPA in the sediment. Generally, dilution with assay buffer easily and effectively reduces or eliminates the matrix effect in immunoassays. However, at the expense of sensitivity, the developed BLEIA based on NB/Nluc is not sensitive enough to detect trace TBBPA in sediment.

**Expression and Characterization of Nanobody/C4BP/Nanoluciferase Fusion.** The affinity of the binder is a key

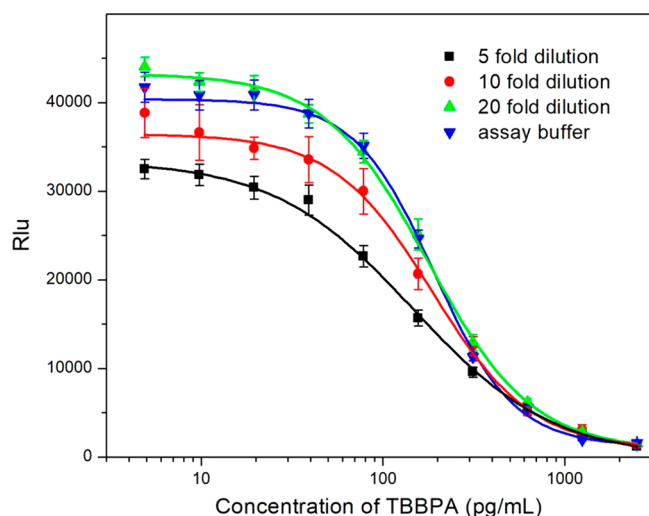


**Figure 2.** Matrix effect of sediment sample in BLEIA based on NB/Nluc including four standard curves of extracted solution tested in different dilutions (5-, 10-, 20-fold and assay buffer).

factor for sensitivity in an immunoassay. Some reports have already pointed out that the application of multivalent antibody can increase antibody avidity and the corresponding sensitivity of immunoassay.<sup>24</sup> In the present study, the nanobody against TBBPA was fused to the N-terminal of the C4BP peptide, while nanoluciferase was fused to the C-terminus of C4BP. The designed C4BP gene was inserted in the current vector containing the NB/Nluc gene by special primers listed in Table S2. Following the general protocol, this novel heptamer containing two functional domains was expressed in three different *E. coli* hosts, including Tuner (DE3), BL21 (DE3), and Rosetta2 (Gami). As shown in Table S2, there are two cysteines in the protein sequence of C4BP, and the cysteines could form disulfide bonds for cross-linking of each C4BP peptide in the heptamer. We assumed that the protein would self-assemble into NB/C4BP/Nluc heptamer by disulfide bond linkage during expression in *E. coli*. To analyze the multivalency of NB/C4BP/Nluc, SDS-PAGE was run under nonreducing conditions, in which the upper band indicated that the heptamer migrated with a very large molecular mass of about 300 kDa (Figure 3). Meanwhile, running SDS-PAGE under reducing conditions in the presence of 10 mM DTT caused the heptamer to fall apart to about 45 kDa, the size of the monomer. It indicated that the heptamer scaffold was assembled with intermolecular disulfide bonds, which could make the heptameric core structure (C4BP) more stable during the storage.<sup>31</sup> As shown in Figure 3, the expression in three *E. coli* hosts was slightly different, and Rosetta2 (Gami) gave the highest yield of heptamer among the three hosts. According to the manufacturer's protocol, these host strains combine the advantages of the Rosetta 2 and Origami 2 strains to alleviate codon bias and enhance disulfide bond formation when heterologous proteins are expressed in *E. coli*. This feature benefits the formation of heptamer by cross-linking the intermolecular disulfide bonds in C4BP, so the heptamer expressed in this host strain was used for subsequent characterization and assay development. The interactions of monomer NB/Nluc and NB/C4BP/Nluc heptamer with T3-BSA coating antigen were studied with Bio-Layer Interferometry (BLI) (Figure S5). Both NB/Nluc and NB/C4BP/Nluc heptamer specifically recognized T3-BSA coating antigen

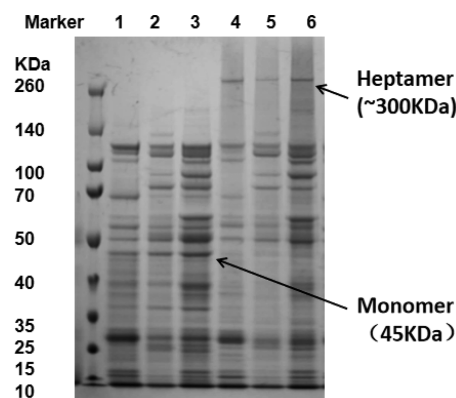


**Figure 3.** SDS-PAGE analysis of expression of the fusion protein. Lane marker: Spectrum multicolor broad-range protein ladder. Lanes 1–3: Whole-cell extract of three *E. coli* hosts under induced conditions in the presence of 10 mM DTT. Lanes 4–6: Whole-cell extract of three *E. coli* hosts under noninduced conditions in the absence of DTT. Lanes 1 and 4, Tuner (DE3); lanes 2 and 5, BL21 (DE3); lanes 3 and 6, Rosetta 2 (Gami).

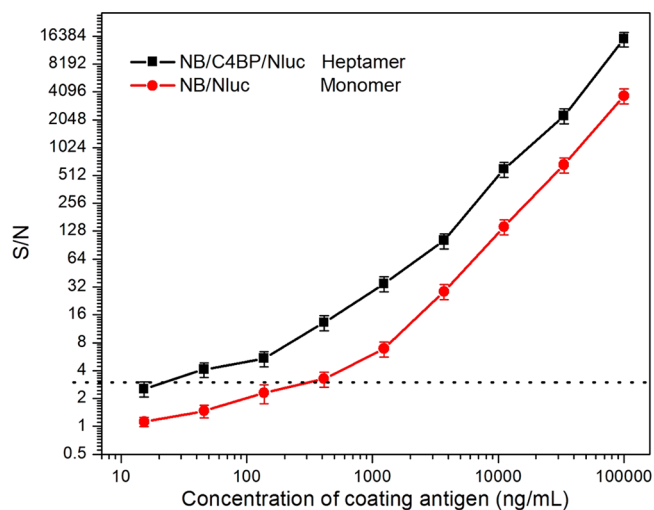
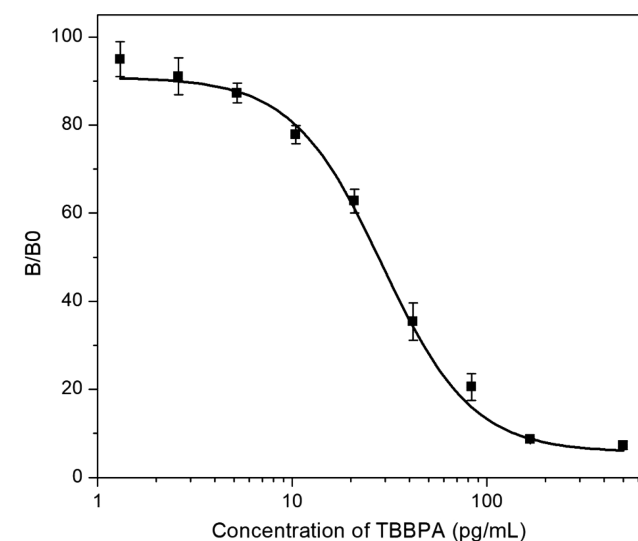
immobilized on the sensor, and the equilibrium dissociation constant  $K_D$  was determined to be around  $1.27 \times 10^{-7}$  and  $1.07 \times 10^{-8}$  M, respectively (Table 1), with a good fit quality ( $R^2 > 0.95$ ). It demonstrated that the avidity of NB/C4BP/Nluc heptamer was increased by almost 10-fold over that of the NB/Nluc monomer. These results showed that the fusion between nanobody and the N-terminus of C4BP peptide enhances the affinity of the nanobody remarkably.

**One-Step BLEIA Based on Nanobody Nanoluciferase Heptamer Fusion.** The NB/C4BP/Nluc heptamer and NB/Nluc were both able to bind to T3-BSA immobilized on the sensor in the BLI test. To compare their performance in immunoassay, two nanobody/nanoluciferase fusions were applied to detect a series of diluted coating antigen T3-BSA coated on the plate. The potency curve was fitted by plotting the luminescence signal response against the concentration of the T3-BSA. The cutoff value in the potency curve was calculated as the concentration with the formula  $S/N > 3$ . As shown in Figure 4, the NB/C4BP/Nluc heptamer fusions showed higher sensitivity with the cutoff of 40 ng/mL T3-BSA, while the cutoff is about 400 ng/mL T3-BSA for monomer NB/Nluc. The results proved that heptamer is a stronger binder against T3-BSA than the monomer. This may be related to the affinity improvement because of multivalent binding interaction, and also to the multivalent tracer, which enlarged the signal amplification. The assay concentration of coating antigen and NB/C4/Nluc was optimized by checkerboard titration, in which the concentrations of both reagents decreased gradually. As shown in Figure 5, one-step BLEIA based on NB/C4BP/Nluc was found to be ultrasensitive to detect a trace level of TBBPA, with an  $IC_{50}$  value of 28.9 pg/mL and LOD of about 2.5 pg/mL in assay buffer. The sensitivity of one-step BLEIA based on heptamer NB/C4BP/Nluc had been improved almost 7-fold as compared to that on monomer NB/Nluc ( $IC_{50}$  value of 187 pg/mL).

As proof of the concept, the C4BP as a linker can be used to generate NB/C4BP/Nluc heptamer fusion; in contrast, the traditional “(GGGG)<sup>2</sup>” linker could only generate NB/Nlu monomer fusion. This novel design integrated seven nanobody binders and seven tracers for developing an improved bioluminescence immunoassay on the first try. In our previous

**Table 1.**  $K_D$  Value of NB/Nluc Monomer and NB/C4BP/Nluc Heptamer Determined by BLI against the Immobilized Coating Antigen on the Sensor

sample	response	$K_D$ (M)	$K_{on}$ (1/M·s)	$K_{dis}$ (1/s)	$R^2$
monomer	0.1567	$1.27 \times 10^{-7}$	$7.37 \times 10^3$	$9.34 \times 10^{-4}$	0.9879
heptamer	0.2225	$1.07 \times 10^{-8}$	$9.42 \times 10^4$	$1.01 \times 10^{-3}$	0.9884

**Figure 4.** Potency test (S/N ratio) of monomer NB/Nluc and heptamer NB/C4BP/Nluc. S represents the bioluminescent signal in the presence of coating antigen, and N represents the signal in the absence of coating antigen.**Figure 5.** Standard curve of one-step BLEIA based on heptamer binder/tracer.

study, the same nanobody was fused with alkaline phosphatase (AP), which forms a dimer NB–AP fusion.<sup>15</sup> The reported ELISA-based dimer fusion has an  $IC_{50}$  of 200  $\mu\text{g/mL}$ ; it is less sensitive than BLEIA based on heptamer fusion and even the monomer fusion. In conclusion, the BLEIA based on heptamer NB/C4BP/Nluc fusion demonstrated the best sensitivity among other reported immunoassays for TBBPA. Thus, it could serve as an ultrasensitive assay to detect the trace TBBPA in the complicated matrix.

**Detection of TBBPA in Sediment.** BLEIA based on heptamer NB/C4BP/Nluc was performed to analyze TBBPA in the spiked sediment samples to evaluate the reliability of the method. Before the spiking and recovery study, undetectable TBBPA in the sediment sample was supported by LC–MS/MS analysis. Five doses of TBBPA (500, 1000, 1500, 3000, and 4000  $\mu\text{g}$ ) were spiked into 1 g of dry sediment samples. The sediment sample was extracted with 5-fold volume solution and diluted with assay buffer in 20-fold, which has been shown as an effective method to eliminate matrix effect in immunoassays. The diluted extracts were subjected to the BLEIA based on both NB/Nluc and NB/C4BP/Nluc and also measured by LC–MS/MS for validation. In this work, the bioluminescent detection mode showed significant advantages in terms of sensitivity in comparison with conventional colorimetric techniques. The NB/Nluc fusion and NB/C4BP/Nluc both demonstrated excellent sensitivity in the detection of trace TBBPA in sediment. As shown in Table 2, a sensitive BLEIA based on an NB/Nluc fusion protein could be applied to detect trace TBBPA as low as 3000  $\mu\text{g/g}$  in sediment samples. However, trace TBBPA 500  $\mu\text{g/g}$  in sediment samples could not be detected by BLEIA on the basis of the NB/C4BP/Nluc reagent. Because of the complex of multivalent binder and tracer, the LOD of heptamer BLEIA was nearly 7 times lower than that of the monomer BLEIA. The high sensitivity of heptamer BLEIA overcomes the negative impact of dilution on the sensitivity. Even with 100-fold dilution in the sediment sample, as low as 500  $\mu\text{g/g}$  TBBPA in sediment was still detectable by BLEIA based on heptamer fusion. The average recoveries for BLEIA ranged from 92% to 103%. The results were also highly consistent with those detected by traditional LC–MS/MS, which indicated that the developed one-step BLEIA is reliable, accurate, and reproducible. Therefore, it can

**Table 2.** Detection of Spiked TBBPA in Sediment Samples with Developed Monomer BLEIA (Monomer) and BLEIA (Heptamer) as Compared to LC–MS/MS

spiked ( $\mu\text{g/g}$ )	BLEIA (monomer)		BLEIA (heptamer)		LC–MS/MS
	found ( $\mu\text{g/g}$ )	recovery (%)	found ( $\mu\text{g/g}$ )	recovery (%)	found ( $\mu\text{g/g}$ )
4500	$4298 \pm 176$	96	$4175 \pm 61$	93	$4255 \pm 213$
3000	$2837 \pm 95$	95	$2901 \pm 99$	97	$2921 \pm 87$
1500	ND		$1421 \pm 32$	95	$1326 \pm 69$
1000	ND		$1028 \pm 79$	103	$1089 \pm 40$
500	ND		$462 \pm 24$	92	$453 \pm 18$
0	ND		ND		ND

be utilized as an important tool for the detection of TBBPA in sediment samples.

## CONCLUSION

To monitor trace levels of TBBPA in sediment, we developed an ultrasensitive BLEIA based on an anti-TBBPA nanobody in a different fusion format. First, the nanobody was fused with nanoluciferase. The resulting one-step BLEIA based on this dual-functional reagent greatly improved the sensitivity as compared to the classic two-step ELISA. To further enhance the sensitivity of the one-step BLEIA, an assembled peptide was applied to form a nanobody/nanoluciferase heptamer. Because of its great binding capacity and signal amplification, this novel dual-functional reagent resulted in a huge enhancement of sensitivity in one-step BLEIA. The proposed assay was further applied in the detection of trace TBBPA in the sediment sample, and the recovery rate was within 92–103%, which indicated that it is an efficient tool in environmental monitoring.

## ASSOCIATED CONTENT

### Supporting Information

The Supporting Information is available free of charge at <https://pubs.acs.org/doi/10.1021/acs.analchem.0c01908>.

Assay format two-step nanobody-based ELISA; vector construction of NB/Nluc fusion; assay format of one-step BLEIA based on NB/Nluc; BLI affinity test of NB/Nluc and NB/C4BP/Nluc; primers and sequence of monomer NB/Nluc fusion; primers and sequence of heptamer NB/C4BP/Nluc fusion; and the optimized conditions of LC–MS/MS (PDF)

## AUTHOR INFORMATION

### Corresponding Author

**Bruce D. Hammock** – Department of Entomology and Nematology and UCD Comprehensive Cancer Center, University of California, Davis, California 95616, United States; [orcid.org/0000-0003-1408-8317](https://orcid.org/0000-0003-1408-8317); Email: [bdhammock@ucdavis.edu](mailto:bdhammock@ucdavis.edu)

### Authors

**Zhenfeng Li** – Department of Entomology and Nematology and UCD Comprehensive Cancer Center, University of California, Davis, California 95616, United States; [orcid.org/0000-0002-6068-6548](https://orcid.org/0000-0002-6068-6548)

**Yi Wang** – Department of Entomology and Nematology and UCD Comprehensive Cancer Center, University of California, Davis, California 95616, United States; Department of Pesticides Science, School of Resources and Environment, Anhui Agricultural University, Hefei 230036, China; [orcid.org/0000-0001-8043-4869](https://orcid.org/0000-0001-8043-4869)

**Natalia Vasylieva** – Department of Entomology and Nematology and UCD Comprehensive Cancer Center, University of California, Davis, California 95616, United States

**Debin Wan** – Department of Entomology and Nematology and UCD Comprehensive Cancer Center, University of California, Davis, California 95616, United States

**Zihan Yin** – Department of Entomology and Nematology and UCD Comprehensive Cancer Center, University of California, Davis, California 95616, United States

**Jiexian Dong** – Shenzhen Forward Pharma Co., Ltd., Shenzhen 518057, China

Complete contact information is available at: <https://pubs.acs.org/10.1021/acs.analchem.0c01908>

## Author Contributions

<sup>||</sup>Z.L. and Y.W. contributed equally to this work.

## Author Contributions

Z.L., Y.W., and B.D.H. designed the research; Z.L., D.W., Z.Y., and J.D. performed the experiment; and Z.L., Y.W., N.V., and B.D.H. analyzed the data and wrote the paper.

## Notes

The authors declare no competing financial interest.

## ACKNOWLEDGMENTS

We are thankful for the support from the National Institute of Environmental Health Science (NIEHS) Superfund Research Program (P42ES004699), NIEHS RIVER Award R35 ES030443-01, the National Academy of Sciences (NAS, subaward no. 2000009144), and the China Scholarship Council (CSC, no. 201908340037). The article is derived from the subject data funded in part by NAS and USAID, and any opinions, findings, conclusions, or recommendations expressed in such articles are those of the authors alone and do not necessarily reflect the views of USAID or NAS.

## REFERENCES

- (1) Malkoske, T.; Tang, Y.; Xu, W.; Yu, S.; Wang, H. *Sci. Total Environ.* **2016**, 569–570, 1608–1617.
- (2) Abou-Elwafa Abdallah, M. *Environ. Int.* **2016**, 94, 235–250.
- (3) Zhu, M. Q.; Xu, Y. M.; Sang, L. F.; Zhao, Z. Y.; Wang, L. J.; Wu, X. Q.; Fan, F. G.; Wang, Y.; Li, H. *Environ. Pollut.* **2020**, 256, 113427.
- (4) Hays, S. M.; Kirman, C. R. *Regul. Toxicol. Pharmacol.* **2019**, 102, 108–114.
- (5) Gustavsson, J.; Wiberg, K.; Ribeli, E.; Nguyen, M. A.; Josefsson, S.; Ahrens, L. *Sci. Total Environ.* **2018**, 625, 1046–1055.
- (6) Wang, Y.; Wang, L. J.; Zhu, M. Q.; Xue, J. Y.; Hua, R. M.; Li, Q. X. *J. Lumin.* **2019**, 205, 210–218.
- (7) Malysheva, S. V.; Gosciny, S.; Malarvannan, G.; Poma, G.; Andjelkovic, M.; Voorspoels, S.; Covaci, A.; Van Looc, J. *Food Addit. Contam., Part A* **2018**, 35, 292–304.
- (8) Yu, Y.; Zhu, X.; Zhu, J.; Li, L.; Zhang, X.; Xiang, M.; Ma, R.; Yu, L.; Yu, Z.; Wang, Z. *Ecotoxicol. Environ. Saf.* **2019**, 176, 364–369.
- (9) Gao, W.; Tian, Y.; Liu, H.; Cai, Y.; Liu, A.; Yu, Y. L.; Zhao, Z.; Jiang, G. *Anal. Chem.* **2019**, 91, 772–775.
- (10) Wang, L. J.; Wu, X. Q.; Yang, Y. N.; Liu, X. N.; Zhu, M. Q.; Fan, S. S.; Wang, Z.; Xue, J. Y.; Hua, R. M.; Wang, Y.; Li, Q. X. *Sci. Total Environ.* **2019**, 686, 1039–1048.
- (11) Xu, T.; Wang, J.; Liu, S. Z.; Lu, C.; Shelver, W. L.; Li, Q. X.; Li, J. *Anal. Chim. Acta* **2012**, 751, 119–127.
- (12) Bever, C. S.; Dong, J. X.; Vasylieva, N.; Barnych, B.; Cui, Y.; Xu, Z. L.; Hammock, B. D.; Gee, S. J. *Anal. Bioanal. Chem.* **2016**, 408, 5985–6002.
- (13) Wang, J.; Bever, C. R.; Majkova, Z.; Dechant, J. E.; Yang, J.; Gee, S. J.; Xu, T.; Hammock, B. D. *Anal. Chem.* **2014**, 86, 8296–8302.
- (14) Sheng, Y. M.; Wang, K.; Lu, Q. Z.; Ji, P. P.; Liu, B. Y.; Zhu, J. H.; Liu, Q. Y.; Sun, Y. L.; Zhang, J. F.; Zhou, E. M.; Zhao, Q. J. *Nanobiotechnol.* **2019**, 17, 35–50.
- (15) Wang, J.; Majkova, Z.; Bever, C. R.; Yang, J.; Gee, S. J.; Li, J.; Xu, T.; Hammock, B. D. *Anal. Chem.* **2015**, 87, 4741–4748.
- (16) Fu, H. J.; Wang, Y.; Xiao, Z. L.; Wang, H.; Li, Z. F.; Shen, Y. D.; Lei, H. T.; Sun, Y. M.; Xu, Z. L.; Hammock, B. *Ecotoxicol. Environ. Saf.* **2020**, 188, 109904–109911.
- (17) He, T.; Wang, Y. R.; Li, P. E.; Zhang, Q.; Lei, J. E.; Zhang, Z. E.; Ding, X. X.; Zhou, H. Y.; Zhang, W. *Anal. Chem.* **2014**, 86, 8873–8880.
- (18) He, J.; Tian, J.; Xu, J.; Wang, K.; Li, J.; Gee, S. J.; Hammock, B. D.; Li, Q. X.; Xu, T. *Anal. Bioanal. Chem.* **2018**, 410, 6633–6642.

- (19) Golet, E. M.; Strehler, A.; Alder, A. C.; Giger, W. *Anal. Chem.* **2002**, *74*, 5455–5462.
- (20) Le, H. T.; Szurdoki, F.; Szekacs, A. *Pest Manage. Sci.* **2003**, *59*, 410–416.
- (21) Lima, D. L. D.; Silva, C. P.; Schneider, R. J.; Esteves, V. I. *Talanta* **2011**, *85*, 1494–1499.
- (22) Huo, J.; Li, Z.; Wan, D.; Li, D.; Qi, M.; Barnych, B.; Vasylieva, N.; Zhang, J.; Hammock, B. D. *J. Agric. Food Chem.* **2018**, *66*, 11284–11290.
- (23) Ren, W.; Li, Z.; Xu, Y.; Wan, D.; Barnych, B.; Li, Y.; Tu, Z.; He, Q.; Fu, J.; Hammock, B. D. *J. Agric. Food Chem.* **2019**, *67*, 5221–5229.
- (24) Soukka, T.; Harma, H.; Paukkunen, J.; Lovgren, T. *Anal. Chem.* **2001**, *73*, 2254–2260.
- (25) Safenkova, I. V.; Zherdev, A. V.; Dzantiev, B. B. *J. Immunol. Methods* **2010**, *357*, 17–25.
- (26) Nunez-Prado, N.; Compte, M.; Harwood, S.; Alvarez-Mendez, A.; Lykkemark, S.; Sanz, L.; Alvarez-Vallina, L. *Drug Discovery Today* **2015**, *20*, 588–594.
- (27) Zhang, J. B.; Tanha, J.; Hiram, T.; Khieu, N. H.; To, R.; Hong, T. S.; Stone, E.; Brisson, J. R.; MacKenzie, C. R. *J. Mol. Biol.* **2004**, *335*, 49–56.
- (28) Stone, E.; Hiram, T.; Tanha, J.; Tong-Sevinc, H.; Li, S. H.; MacKenzie, C. R.; Zhang, J. B. *J. Immunol. Methods* **2007**, *318*, 88–94.
- (29) Zhu, X.; Wang, L.; Liu, R.; Flutter, B.; Li, S.; Ding, J.; Tao, H.; Liu, C.; Sun, M.; Gao, B. *Immunol. Cell Biol.* **2010**, *88*, 667–675.
- (30) Fan, K.; Jiang, B.; Guan, Z.; He, J.; Yang, D.; Xie, N.; Nie, G.; Xie, C.; Yan, X. *Anal. Chem.* **2018**, *90*, 5671–5677.
- (31) Hofmeyer, T.; Schmelz, S.; Degiacomi, M. T.; Dal Peraro, M.; Daneschdar, M.; Scrima, A.; van den Heuvel, J.; Heinz, D. W.; Kolmar, H. *J. Mol. Biol.* **2013**, *425*, 1302–1317.
- (32) Libyh, M. T.; Goossens, D.; Oudin, S.; Gupta, N.; Dervillez, X.; Juszcak, G.; Cornillet, P.; Bougy, F.; Reveil, B.; Philbert, F.; Tabary, T.; Klatzmann, D.; Rouger, P.; Cohen, J. H. M. *Blood* **1997**, *90*, 3978–3983.
- (33) Valldorf, B.; Fittler, H.; Deweid, L.; Ebenig, A.; Dickgiesser, S.; Sellmann, C.; Becker, J.; Zielonka, S.; Empting, M.; Avrutina, O.; Kolmar, H. *Angew. Chem., Int. Ed.* **2016**, *55*, 5085–5089.
- (34) Janatova, J.; Reid, K. B. M.; Willis, A. C. *Biochemistry* **1989**, *28*, 4754–4761.